Finite Element Model and Experimental Analysis of Crack–Inclusion Interaction

R. LI,[1] S. WU,[1,*] E. IVANOVA,[1] A. CHUDNOVSKY,[1] K. SEHANOBISH,[2] and C. P. BOSNYAK[2]

[1]Department of Civil Engineering, Mechanics and Metallurgy, University of Illinois at Chicago, Box 4348, Chicago, Illinois 60680, and [2]The Dow Chemical Company, 2301 N. Brazosport Blvd., Freeport, Texas 77541

SYNOPSIS

One of the key requirements for developing tough multiphase blend systems, for example, selecting the type of discrete phases (hard or soft) in a polymer matrix, is the ability to predict the fracture path. Most of these selections rely heavily on prior experience or on intuitive rationale. There are few mathematical guidelines for the materials scientists who are designing new multiphase systems. This article is designed mainly to provide such insight through the development of a theoretical model and through experimental observation. A finite element model has been used to predict the crack velocity and the crack path for a crack that approaches and penetrates a hard or a soft inclusion. A novel experimental approach is then utilized to verify these predictions by introducing hard and soft circular domains in poly(ethylene-*co*-carbon monoxide) specimens by selective photodegradation. © 1993 John Wiley & Sons, Inc.

INTRODUCTION

One of the key requirement for developing a tough multiphase blend system is the ability to predict the fracture path before selecting the type of discrete phases (hard or soft) in a polymer matrix. Most of these selections have relied heavily on prior experiences or on intuitive rationale. There are only a few mathematical guidelines for the materials scientist who is designing new multiphase systems. We have found that the difficult task of designing these systems can be tackled with relatively simple experimental and numerical models. Several researchers addressed this type of problem by solving sets of integral equations.[1–4] Often, the results of these analyses are difficult to use because of a lack of experimental verification. The problem of a crack penetrating into a soft inclusion was also addressed by various authors.[5–7] The inclusion problem, with a crack crossing the boundary, was discussed for a crack with a fixed length crossing the boundary in various locations.[4] Some experimental studies, using photoelasticity, have been attempted by several other researchers.[8,9] However, these reports mainly address the stress field in the vicinity of a crack interacting with an inclusion. Knowledge of the stress field alone does not provide adequate insight into the fracture of such a system, especially for a crack approaching and penetrating into a stiff/soft inclusion. This article describes the fracture mechanism, based on a theoretical model, combined with a specially designed experimental setup.

FINITE ELEMENT MODELLING

Finite element solutions for a crack that is approaching and penetrating soft and stiff inclusions in a finite geometry specimen are not available in the literature. Although there are analytical solutions for crack–inclusion interaction problems,[2,3] and the problem of a crack with a fixed length in various locations, crossing the boundary of inclusion, has been discussed in Ref. 4, most of these solutions are not concerned with a crack approaching and penetrating an inclusion. Here, a two dimensional (2-D) finite element method is used to address the crack–inclusion interaction problem. The eight-

* To whom correspondence should be addressed.

Journal of Applied Polymer Science, Vol. 50, 1233–1238 (1993)
 CCC 0021-8995/93/071233-06

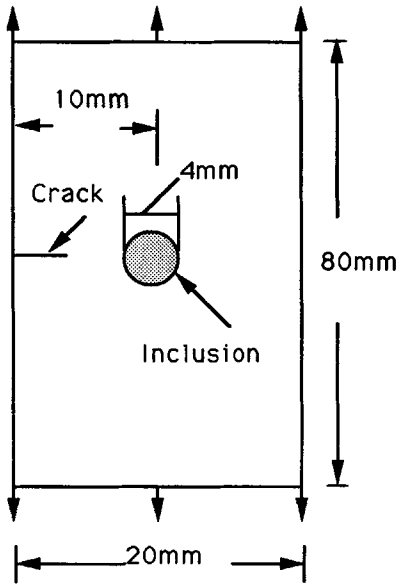

Figure 1 The sketch of specimen geometry and location of inclusion.

noded isoparametric element is used for the analysis. The element, with the shift of the midpoint to the quarterpoint, is used to simulate singularity at the crack tip. The software showed good agreement with known analytical and numerical solutions for specific crack problems in an elastic medium.[10,11] After establishing the validity of the software, it was applied to address the problem of a crack that is approaching and penetrating soft and hard inclusions in a finite geometry specimen. The geometry of the specimen is presented in Figure 1.

The results of the computation, in terms of the energy release rate (ERR) normalized by the energy release rate, G_I^0, for the same specimen configuration with no inclusion, are shown in Figures 2 and 3 as a function of distance from the center of the inclusion, normalized by the radius of the inclusion. For the case of a soft inclusion, the energy release rate increases noticeably as the crack approaches the boundary from a distance approximately 1.5 times the diameter of the inclusion (Fig. 2). The energy

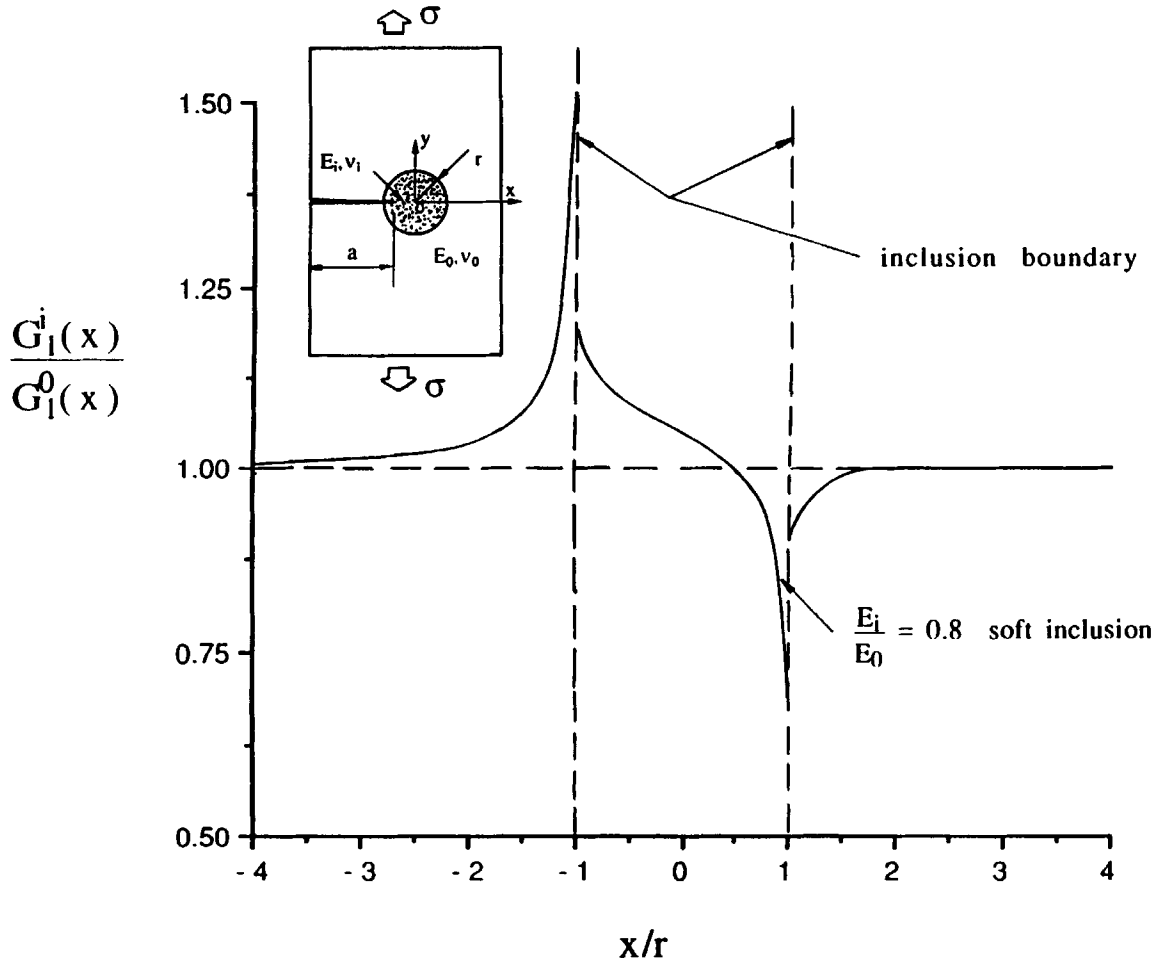

Figure 2 The influence of crack–soft inclusion interaction on the normalized energy release rate of the crack tip.

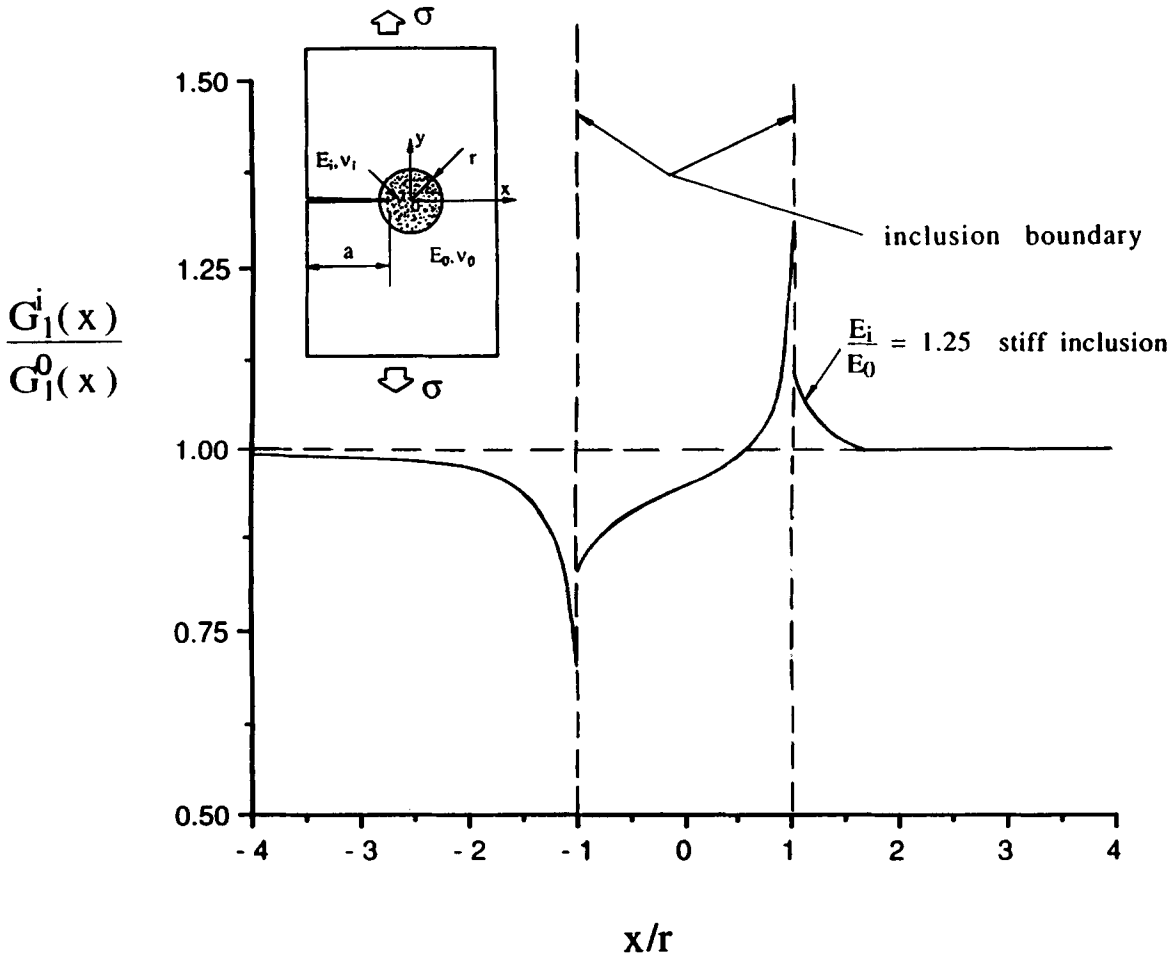

Figure 3 The influence of crack–stiff inclusion interaction on the normalized energy release rate of the crack tip.

release rate decreases during the period of crack penetration through the inclusion as a result of the shielding effect of a soft inclusion. After the crack reaches the boundary, the energy release rate increases once again and quickly reaches the value for an interaction-free crack at $x/r = 1.5$.

In the case of stiff inclusion, the energy release rate decreases, which is similar to the previous case, up to the boundary of the inclusion (Fig. 3). The energy release rate then increases during crack penetration through the stiff inclusion. After the crack passes through the inclusion, the energy release rate decreases to the level of the inclusion free crack. Assuming, for a crack with a small process zone, that the ERR correlates with crack speed, one may anticipate an acceleration of the crack towards the boundary for the soft inclusion, followed by a decrease of crack speed inside the inclusion. After the crack leaves the inclusion, the speed should rise to the speed of an inclusion-free crack. In the same way, one may expect a decrease in crack speed towards the boundary for a stiff inclusion. These predictions are compared with experimental observations reported in the following section.

EXPERIMENTAL INVESTIGATIONS

In order to create a stiff and soft inclusion in a polymer matrix at specific locations, region selective UV degradation was utilized. This appears to be a simpler approach than embedding hard and soft phases within a matrix. Furthermore, this method avoids the complexity of interface between the inclusion and the matrix. Some investigation was performed on the photodegradation of poly(ethylene-*co*-carbonmonoxide).[12] It was found in those studies that, upon exposing the sample to UV, profuse crosslinking leads to the hardening of the specimen, whether the specimen was under load or not. This method

was applied to create specimens for the present study.

Compression-molded plaques, 0.15 mm in thickness, were prepared from pellets by heating to 190°C under 4 MN/m^2 pressure for 5 min and then they were cooled while maintaining the pressure. Rectangular specimens with dimensions 20 × 80 mm were punched from the plaques. First, several specimens were uniformly degraded to determine the material properties, such as modulus and the fracture toughness. It was found that the ratio of the Young's modulus of degraded material, E_i, over the original material, E_o, is about 1.2, while the ratio of the fracture toughness of degraded over that of the original is about 0.1. This means that the influence of UV on the fracture toughness is more significant than on the elastic properties. After this was established, the soft inclusion in a relatively hard matrix was prepared by covering a circular region, with a diameter of 4 mm, using a polymer composite capable of totally shielding the incoming UV radiation. In order to produce the stiff inclusion, the specimen was covered entirely except for a circular region with a diameter of 4 mm. After the radiation treatment, a notch was introduced in the line of symmetry of the sample, passing through the center of the inclusions (Fig. 1). Next, a fatigue experiment was performed at a maximum stress of $\frac{1}{3}$ the peak stress determined from the monotonic tensile test. A load ratio of 0.125 and a frequency of 1 Hz was maintained during the experiment at room temperature.

Figure 4 shows the position of the crack on reaching the boundary of the soft inclusion and Figure 5 shows the crack penetrating through the soft inclusion. The lighter area in the micrograph represents the hard matrix, whereas the relatively darker area represents the soft inclusion. For illustrative purposes, boxes (A) and (B) are placed at the crack face in the hard matrix and the soft inclusion, respectively (Fig. 5). The features at the crack surface, displaying the nature of the crack, are significantly different adjacent to these boxes. While the crack surfaces are clean in the relatively brittle matrix, the crack in the softer inclusion shows signs of yielding (Fig. 5). This observation is further emphasized in Figure 6(A) and (B), which shows the side view of the fracture surface in the hard matrix and the soft inclusion, respectively. Drawn fibers are noticeable in Figure 6(A), confirming ductile crack growth through the soft inclusion.

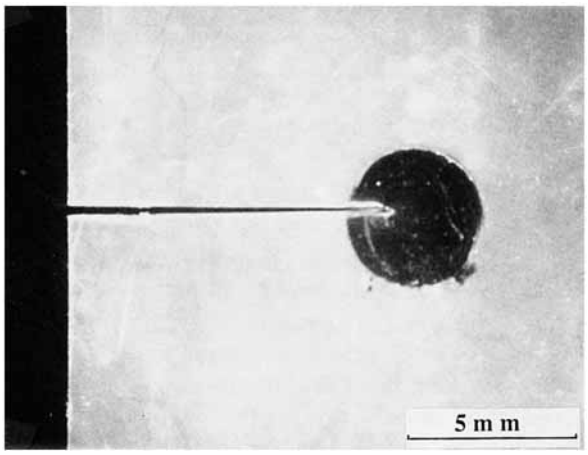

Figure 4 Optical microscopy of the crack, penetrating inside a soft inclusion.

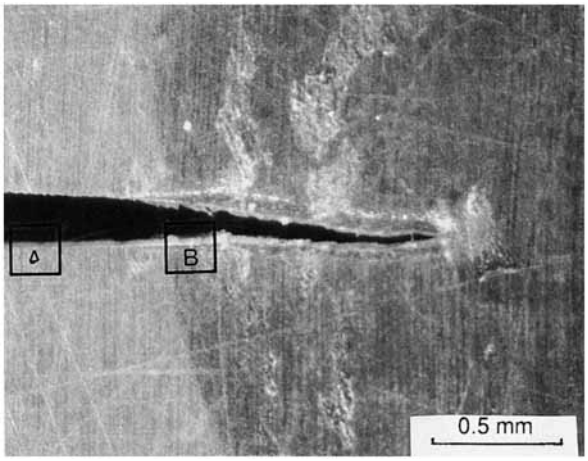

Figure 5 High magnification microscopy of crack, penetrating inside the inclusion.

In order to compare these results with our expectation from the finite element modelling, the crack speed was measured during the whole process. This was monitored using an optical microscope with an attached video system. A representative plot of the crack speed, as a function of crack length, is shown in Figure 7. As anticipated, the crack speed increases up to the boundary of the soft inclusion, followed by a decrease during penetration of the inclusion. However, in these experiments, the effect of the fracture toughness is more significant than demonstrated in the finite element analysis, since the combination of the energy release rate and fracture toughness control the crack propagation process. Catastrophic failure occurs as the crack crosses about 80% of the soft inclusion, because of the proximity of the crack tip to the boundary. No failure criterion was introduced in the mathematical model, and consequently no comparison can be made with the model after this point.

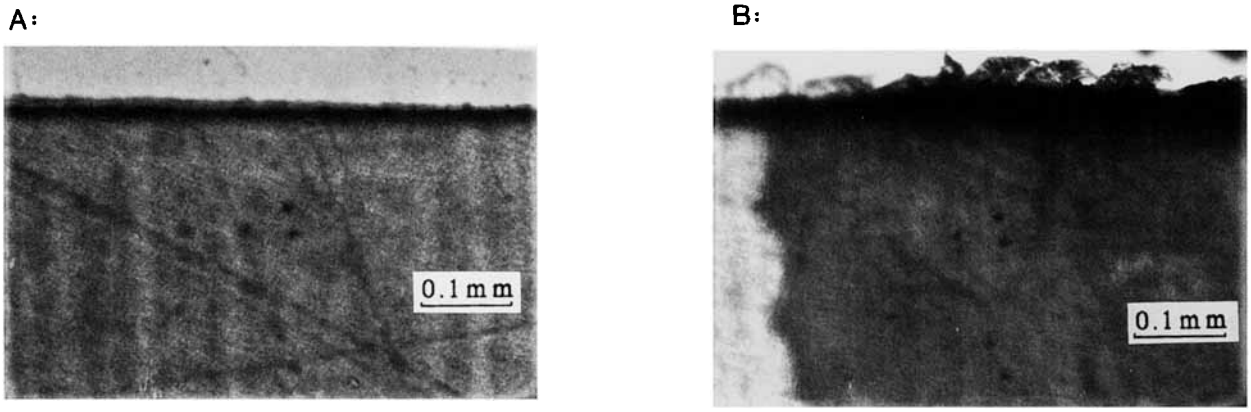

Figure 6 Side view of the fracture surface in region (A) and (B) in Figure 5.

A correlation between the experimental observation of the crack speed, da/dt, and the calculated energy release rate, G_1, is shown in Figure 8. It can be seen that before the crack crosses the inclusion boundary, both da/dt and G_1 increase. However, after the crack penetrates the inclusion, although the energy release rate still increases due to the increase of the crack length, the crack speed drops dramatically. The reason for the crack speed decrease is primarily due to the increase of toughness of the soft inclusion. The process zone [Fig. 6(B)], developed during crack penetration in the soft inclusion, provides resistance to crack growth. Linear elastic finite element modelling is not valid any longer inside the soft inclusion, and thus crack layer modelling would be necessary.[13]

Based on the 2-D finite element model, it can be speculated that, for the case of stiff inclusion, a decrease in energy release rate could result in a possible crack arrest. Experimental results indicate that, before the crack could advance towards the boundary, a through crack suddenly appears inside the stiff inclusion (see Fig. 9). This phenomena is within the expectation of the model if one considers that the hardening of the inclusion has resulted in a decrease in fracture toughness. The experiment was discontinued after the large crack appeared inside the stiff inclusion. In addition, the crack speed was not considered in this case, since the experiment switched to a complex crack interaction problem.

CONCLUSIONS

1. A 2-D finite element method has been used to model crack interaction with, and penetration in, stiff and soft inclusions. Expec-

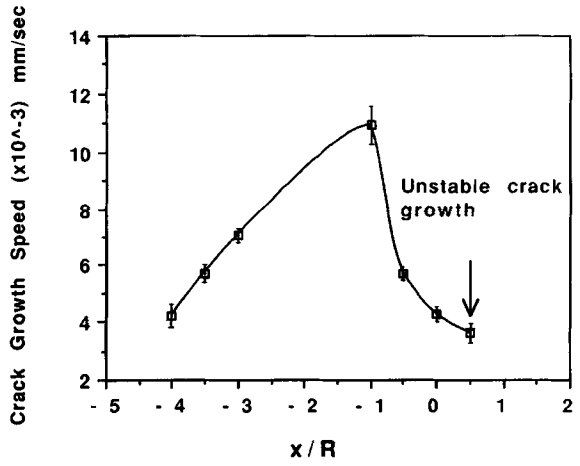

Figure 7 Experimental observation of the crack growth speed when the crack, approaching and penetrating the soft inclusion versus the normalized crack length, x/R.

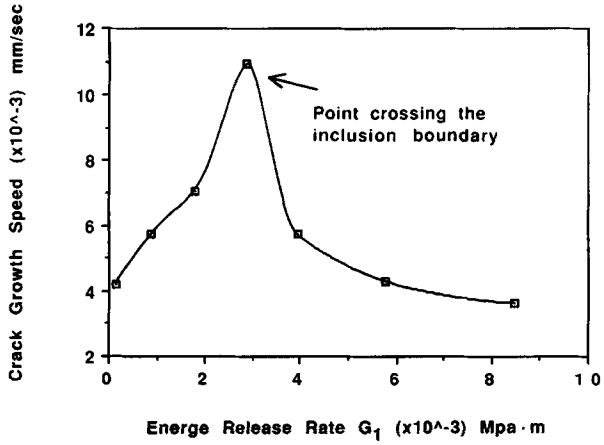

Figure 8 The correlation between the energy release rate and the crack growth speed of a crack interacting with a soft inclusion.

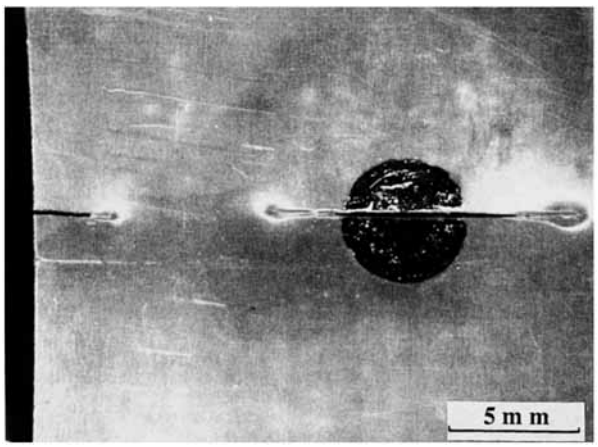

Figure 9 Optical microscopy of the crack, penetrating inside a stiff inclusion.

tations from the model agree well with experimental observations of a crack propagating in a poly(ethylene-*co*-carbon monoxide), containing stiff and soft inclusions.

2. Crack interaction with a soft or stiff inclusion significantly influence the fracture path.
3. A novel technique has been developed to create experimental models of crack–inclusion interactions by selectively photodegrading specific regions of the polymer. This method can be used effectively to create several levels of rigidity by controlling the radiation time. This approach circumvents the problem of interfacial failure, commonly found with inserts of stiff and soft inclusions.

The authors wish to acknowledge financial support from the Air Force Office of Scientific Research and to acknowledge Dow Chemical Company for providing the materials for this study.

REFERENCES

1. C. Atkinson, *Int. J. Eng. Sci.*, **10**, 127–136 (1972).
2. F. Erdogan, G. D. Gupta, and M. Ratwani, *J. Appl. Mech.*, **41**, 1007–1013, (1974).
3. E. E. Gdoutos, *Fibre Sci. and Tech.*, **15**, 173–185 (1981).
4. F. Erdogan and G. D. Gupta, *Int. J. Fract.*, **11**, 13–27 (1975).
5. J. W. Hutchinson, *Acta Metallurgica*, **35**(7), 1650–1619, (1987).
6. P. S. Steif, *J. Appl. Mech.*, **54**, 87–92 (1987).
7. C. H. Wu, *J. Appl. Mech.*, **55**, 736–738 (1988).
8. B. J. O'Toole and M. H. Santare, *Exper. Mech.*, **30**, 253–257 (1990).
9. P. S. Theocaris and C. B. Demakos, *Int. J. Fract.*, **32**, 71–92 (1986).
10. C. H. Wu, *J. of Elasticity*, **8**(3), 235–257 (1978).
11. H. Tada, P. C. Paris, and G. R. Irwin, *The Stress Analysis of Cracks Handbook*, Del Research, Hellertown, Pennsylvania, 1973.
12. S. Wu, K. Sehanobish, R. P. Markovich, C. P. Bosnyak, and A. Chudnovsky, *ASME Winter Meeting*, Anaheim, California, 1992.
13. A. Chudnovsky, *Crack Layer Theory*, NASA Report CR-174634 (1984).

Received January 28, 1993
Accepted March 30, 1993